Analysis of Refining of Aluminum Using Fractional Solidification with Forced Convection

K.-H. Kim, S.-H. Lee, and D.N. Lee

Segregation of iron atoms during refining of aluminum using the fractional solidification technique has been analyzed. The redistribution of the solute atoms was influenced by the solidification and solid/liquid interface tangential velocities. Aluminum purity increased with decreasing solidification velocity and increasing tangential velocity. The diffusion boundary thickness was inversely proportional to the square root of the tangential velocity in the cylindrical rotating system. Effects of the tangential and solidification velocities on the effective redistribution coefficient were investigated. The calculated refining curves were in good agreement with measured values.

Keywords
aluminum, refining, solidification

1. Introduction

THREE-LAYER electrolytic refining, zone refining, and fractional solidification methods are being used to refine aluminum (Ref 1). The fractional solidification method, which is becoming popular because of its lower energy consumption, is classified into two processes: remelting and forced convection. The remelting process gives rise to refining during solidification and further refining through remelting and removal of higher-solute regions by heating of the refined solid. However, the remelting method has the drawbacks of lower productivity and the necessity of a refined temperature control (Ref 2, 3). The forced convection method offers the advantages of simpler operation and facilities (Ref 4-6). An analysis of the forced convection method has not been made as yet because the process involves complex interactions between solidification and fluid phenomena in molten metal.

In this study, analyses have been made of the effects of solidification velocity and solid/liquid interface tangential velocity on removing a solute element, iron, from aluminum.

2. Experimental Methods

The initial chemical composition of the aluminum used in the experiment is given in Table 1. The experimental setup for refining by the forced convection method is shown in Fig. 1. Aluminum weighing 3 kg was melted in a 2 kW electric furnace. A rotating cooling pipe of high-purity graphite (30 mm OD, 16 mm ID, and 100 mm long), with one end closed, was connected to a direct-current motor by which rotation could be controlled up to 2000 rev/min. A type 304 stainless steel pipe was connected to the graphite pipe. Air was blown into the rotating tube through a gas blowing pipe installed inside the tube, the air flow rate controlled by a flowmeter. The rotating velocity of the cooling graphite pipe, which facilitated solidification and stirring, was measured by a digital tachometer. The melt was held at 660 °C, the melting point of aluminum. The concentration of iron was determined by inductively coupled plasma chemical tests made on samples taken from locations 10 mm below the top surface of the refined solid aluminum.

K.-H. Kim, M/U FAB. Department, Semiconductor R&D, Samsung Electronics, Kyungki-do 449-200, Korea; **S.-H. Lee,** R&E Division, POSCO Engineering & Construction Co., Ltd., Jukdo-2dong, Pohang, Korea; and **D.N. Lee,** Division of Materials Science and Engineering, Seoul National University, Seoul 151-742, Korea.

3. Experimental Results

Figure 2 shows refining ratios (C_s/C_0, with C_s and C_0 being the solute concentration by weight in the solid and the initial solute concentration, respectively) of iron measured at an airflow rate of 70 L/min as a function of distance from the outer surface of the graphite pipe, which rotated at speeds of 500, 1000, and 1500 rev/min. The refining ratio of iron measured at a given rotating velocity decreased to a minimum value and then increased with increasing distance from the outer surface of the graphite pipe. For a given distance from the outer surface, the refining ratio decreased with increasing rotating speed.

Figure 3 shows the refining ratios of iron measured at airflow rates of 35, 70, and 300 L/min as a function of distance from the outer surface of the graphite pipe, which rotated at a speed of 1000 rev/min. The refining ratio of iron measured at a given airflow rate decreased to a minimum value and then increased with increasing distance from the outer surface of the graphite pipe. For a given distance from the surface, the refining ratio decreased with decreasing airflow rate.

4. Discussion

Refining of aluminum using fractional solidification with forced convection is achieved by segregation. Diffusion of solute in the solid is usually neglected compared to its diffusion in

Table 1 Chemical composition of aluminum

Composition, ppm						
Fe	Si	Ti	V	Ga	Cr	Al
1200	300	40	100	180	20	bal

the liquid. The assumptions of no solute diffusion in the solid, local equilibrium of the two phases across the solid/liquid interface, and rapid and complete solute diffusion in the liquid lead to the Scheil equation (Ref 12):

$$C_s = kC_0 (1 - f_s)^{k-1} \quad \text{(Eq 1)}$$

where f_s is the fraction by weight of the solid in the alloy, and k is the equilibrium redistribution coefficient. However, even in the case of severe convection in the liquid, it is difficult to achieve perfect mixing. Burton et al. (Ref 7) took this fact into account by introducing a diffusion boundary layer. They assumed that the solute transport within the diffusion boundary layer is possible only by diffusion and that complete mixing oc-

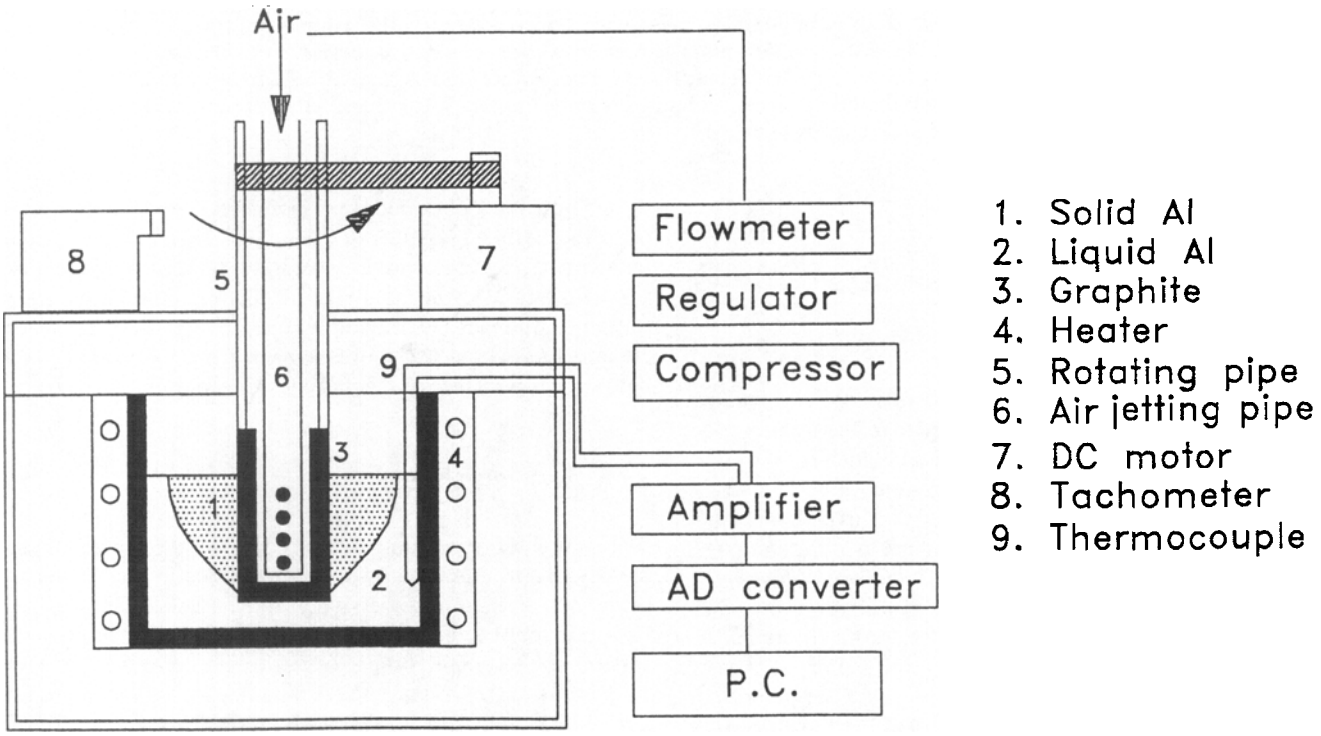

Fig. 1 Schematic of the apparatus

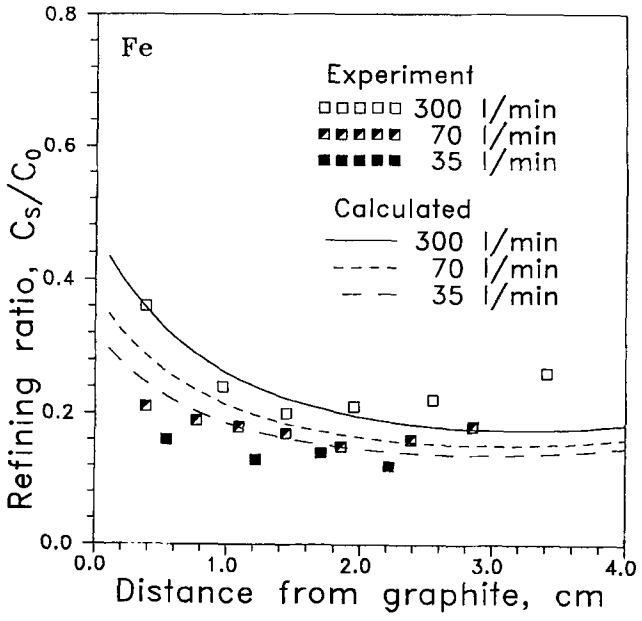

Fig. 2 Effect of rotating speed on refining ratio of iron at an airflow rate of 70 L/min

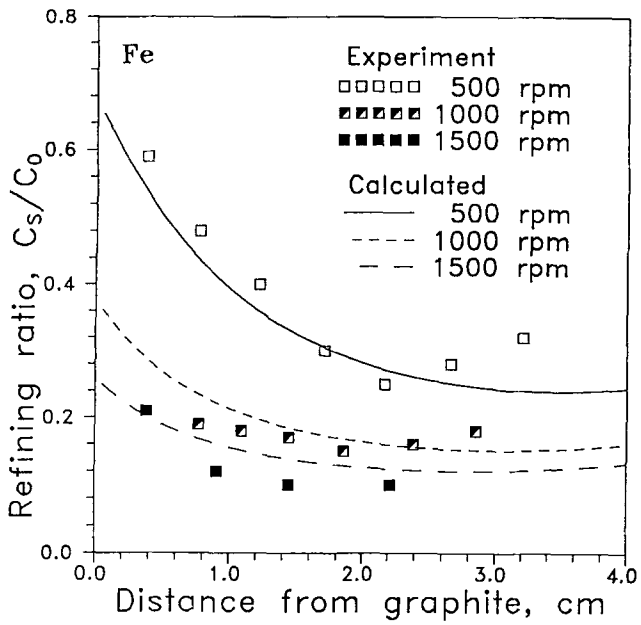

Fig. 3 Effect of air flow rate on refining ratio of iron at a rotating speed of 1000 rev/min

curs in the liquid outside the diffusion layer. The assumption led them to derive an expression called the effective redistribution coefficient:

$$k_e = \frac{k}{k + (1-k)\exp(-R\delta/D_L)} = \frac{k}{k + (1-k)\exp(-\Delta)} \quad \text{(Eq 2)}$$

where R is the solidification velocity, δ is the thickness of the diffusion boundary layer, and D_L is the solute diffusion coefficient in the liquid. The effective redistribution coefficient, k_e, approaches the equilibrium redistribution coefficient, k, with decreasing R and δ. Equation 2, which is rigorously applicable to the planar interface system, can be applied to the cylindrical system as in this study, since the diffusion boundary layer thickness is very small compared to the melt size. The diffusion boundary layer thickness, δ, is known to be independent of the solidification rate at very small solidification rates, but influenced by the solidification rate as the solidification rate increases (Ref 7, 8).

When a melt flows on a plate, δ can be expressed as (Ref 9):

$$\delta = 3D_L^{1/3}\, \nu^{1/6}\, U^{-1/2}\, x^{1/2} \quad \text{(Eq 3)}$$

where ν is the dynamic viscosity, U is the fluid velocity, and x is the distance from the plate edge. In the case of rotational fluid flow as in this study, the quantity of Δ in Eq 2 is assumed to depend on:

$$\Delta = aR^n\, U_s^{-1/2} \quad \text{(Eq 4)}$$

where a and n are constants in a given experimental condition, and U_s is the tangential velocity at the solid/liquid interface. Therefore Eq 2 should be modified to:

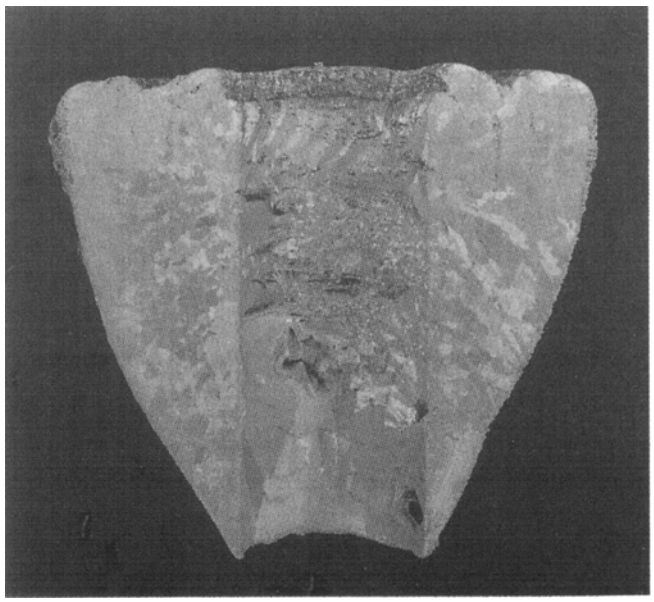

Fig. 4 Longitudinal shape of the specimen solidified under forced convection

$$k_e = \frac{k}{k + (1-k)\exp(-aR^n\, U_s^{-1/2})} \quad \text{(Eq 5)}$$

The Scheil equation (Eq 1) can be modified to:

$$C_s = k_e C_0 (1 - f_s)^{k_e - 1} \quad \text{(Eq 6)}$$

Rearranging Eq 5, we obtain:

$$\ln a + n \ln R = \ln\left[U_s^{1/2} \ln \frac{k_e(1-k)}{k(1-k_e)}\right] \quad \text{(Eq 7)}$$

or

$$\ln a - \frac{1}{2}\ln U_s = \ln\left[R^{-n} \ln \frac{k_e(1-k)}{k(1-k_e)}\right] \quad \text{(Eq 8)}$$

The values of C_s/C_0 are known to depend on r, as shown in Fig. 2 and 3. The value of f_s was measured as a function of r from the specimen shown in Fig. 4, which was obtained at an airflow rate of 70 L/min. The airflow was interrupted for 10 s in intervals of 2 min, and the solidified specimen was sectioned and etched to measure the interrupted marks, from which f_s was evaluated as a function of the radius of solidified body, r (Fig. 5). The best fitting of the data in Fig. 5 yields:

$$f_s = 0.01517\,(r - 1.5)^2 + 0.048422\,(r - 1.5) - 0.001883 \quad \text{(Eq 9)}$$

where r is in centimeters.

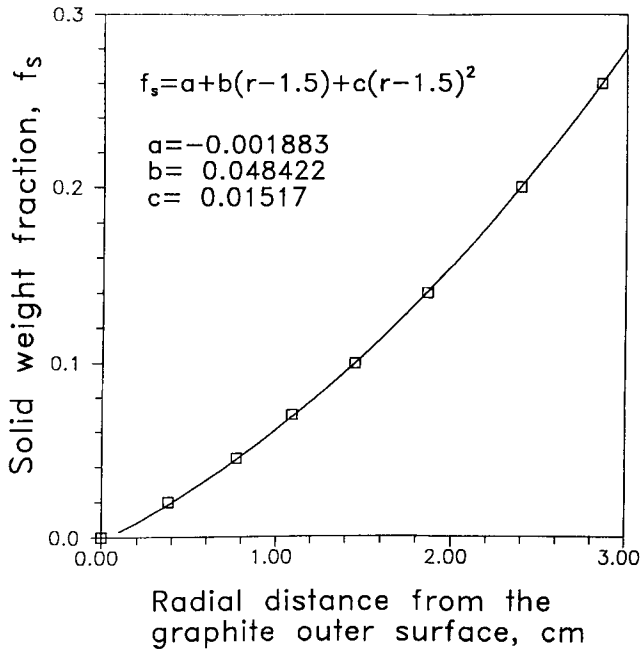

Fig. 5 Relationship between distance from the graphite pipe outer surface and solid weight fraction

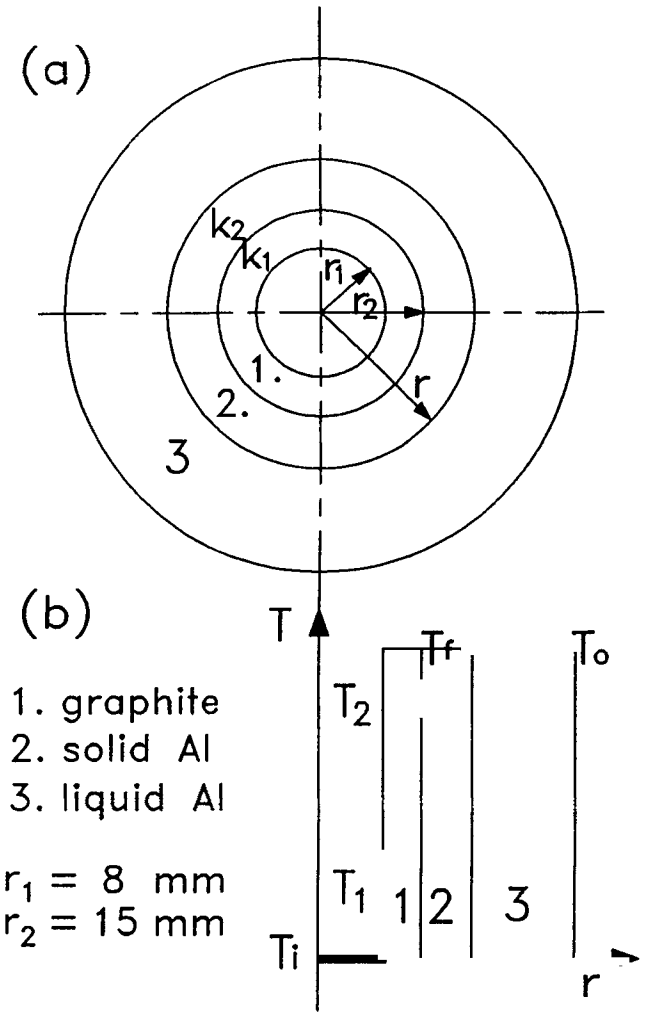

Fig. 6 (a) Schematic shape of the specimen. (b) Temperature profile in the solidification system

Table 2 Thermophysical properties of aluminum and graphite

T_f, °C	660
T_i, °C	20
k_1, W/m · K	17
k_2, W/m · K	210
L, J/m^3	9.5×10^8

The tangential velocity, U_s, at the solid/liquid interface can be calculated from the rotational velocity, f, or the number of rotations per unit time and the value of r, as $U_s = 2\pi rf$. The solidification velocity is difficult to measure. Therefore, the velocity is calculated using a heat-transfer equation. If heat flows uniformly through the cooling graphite pipe from the melt, solidification will proceed radially from the graphite pipe, and the cylindrical coordinate system can be used in the heat-transfer calculation. The temperatures of the solidification front and the melt were assumed to be equal to the melting point of aluminum (660 °C) because of forced convection of the melt. When room-temperature air is blown into the graphite pipe, a temperature distribution from the inside of the pipe to the solid/liquid interface can be drawn as in Fig. 6. Since the heat flow per unit time through each heat resistance is the same, the total heat flux can be expressed as (Ref 10):

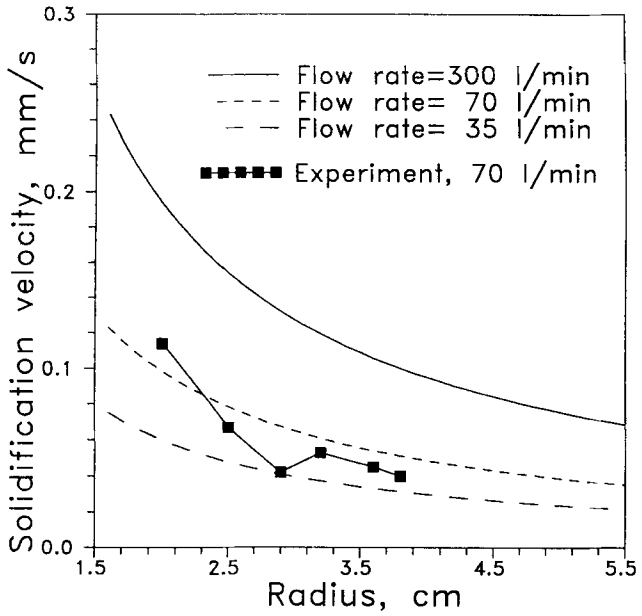

Fig. 7 Variation of solidification velocity with the radius of solidifying aluminum

$$Q = \frac{T_f - T_i}{\frac{1}{2\pi r_1 l \bar{h}_i} + \frac{\ln (r_2/r_1)}{2\pi l k_1} + \frac{\ln (r/r_2)}{2\pi l k_2}} \quad \text{(Eq 10)}$$

where r_1 and r_2 are the inner and outer radii, respectively, of the graphite pipe; T_f and T_i are the melting point of aluminum and room temperature, respectively; k_1 and k_2 are the heat conductivities of graphite and aluminum, respectively; l is the melt height; and $\bar{h}_i$ is the mean heat-transfer coefficient at the air/graphite interface. The heat flux of the solid/liquid interface, q, can be expressed as:

$$q = \frac{Q}{2\pi rl} = \frac{T_f - T_i}{\frac{r}{r_1 \bar{h}_i} + \frac{r \ln (r_2/r_1)}{k_1} + \frac{r \ln (r/r_2)}{k_2}} = L\frac{dr}{dt} \quad \text{(Eq 11)}$$

where L is the latent heat of fusion of aluminum. Therefore, the radial solidification velocity, R, can be expressed as:

$$R = \frac{dr}{dt} = \frac{A}{r(\ln r - B)} \quad \text{(Eq 12)}$$

where

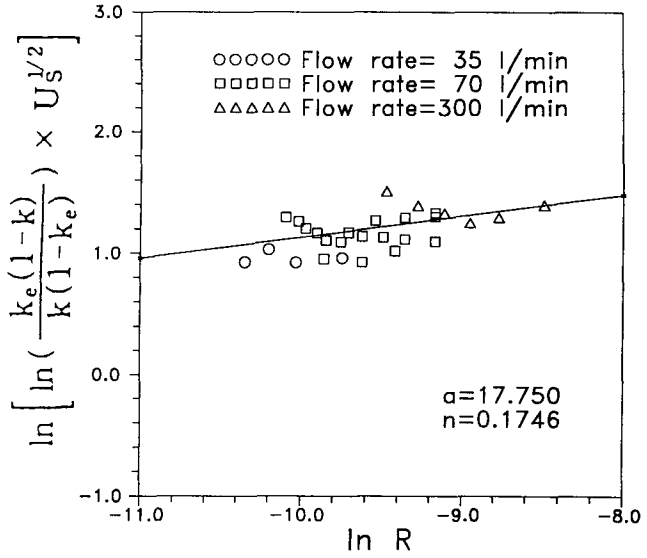

Fig. 8 Relationship between tangential velocity of the rotating solid surface and effective redistribution coefficient of iron for various experimental conditions

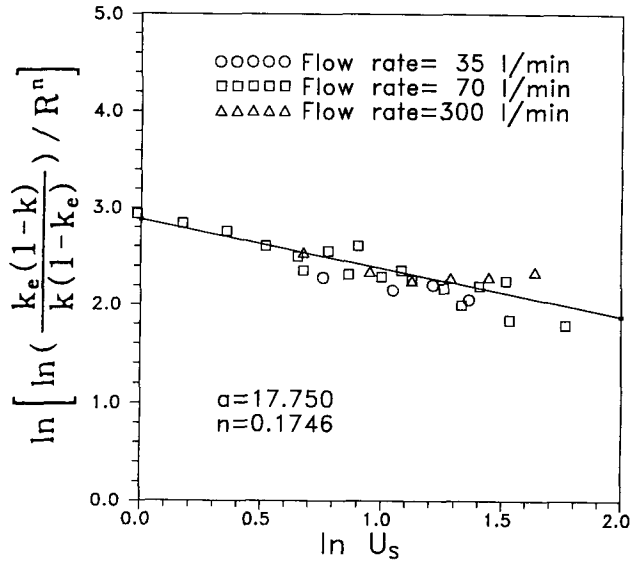

Fig. 9 Relationship between solidification velocity of the rotating solid surface and effective distribution coefficient of iron for various experimental conditions

$$A = \frac{T_f - T_i}{L} k_2$$

$$B = \ln r_2 + \frac{k_2}{k_1} \ln\left(\frac{r_1}{r_2}\right) - \frac{k_2}{r_1 \bar{h}_i}$$

Thermophysical properties used in the calculation are given in Table 2. The value of $\bar{h}_i$ depends on the cooling airflow rate. The value of $\bar{h}_i$ at a given airflow rate was obtained so that it could yield the same f_s as that measured. Thus, the $\bar{h}_i$ values were found to be 238, 409, and 919 W/m^2 · K at airflow rates of 35, 70, and 300 L/min, respectively. Figure 7 shows the solidification velocities calculated using Eq 12 as a function of the radius of the solidified body. The solidification velocity decreases with increasing radius and decreasing airflow rate. The measured values of U_s and k_e, and the calculated values of R, were used to plot in accordance with Eq 7 and 8 (Fig. 8 and 9). The best fitting of the data in Fig. 8 gives n = 0.1746 and a = 17.750. These values give a straight line in Fig. 9, the slope of which is $-1/2$, in good agreement with the theoretical value. The good linear relationship of the data in Fig. 8 and 9 implies that the assumptions made are reasonable.

Once all the values of the parameters in Eq 5 and 6 are known, the effective redistribution coefficient can be calculated as a function of tangential velocity (Fig. 10) or solidification velocity (Fig. 11), within tangible experimental ranges. At a given solidification velocity, the effective redistribution coefficient decreases with increasing tangential velocity. At a given tangential velocity, the redistribution coefficient increases with increasing solidification velocity. The effect of tangential and solidification velocities on the effective redistribution coefficient is shown in Fig. 12. The contour plots of Fig. 12 provide useful information on important process variables of solidification and tangential velocities, allowing a predetermined effective redistribution coefficient to be obtained, which in turn determines refining ratios.

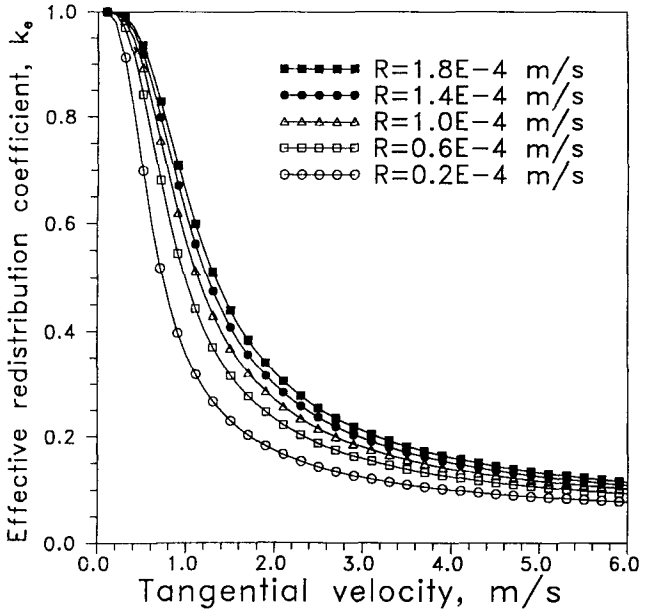

Fig. 10 Effect of tangential velocity on effective redistribution coefficient for various solidification velocities

In order to gauge the applicability of the values of parameters obtained in the analysis, a calculation has been made of the effect of rotation rate of the graphite cooling pipe at an airflow rate on refining of aluminum. The values of R and U_s at a moment are substituted into Eq 5 to give k_e, which is substituted into Eq 6 to yield the refining ratio of iron, C_s/C_0. The calculated results are shown in Fig. 2 and 3 along with the experimental data. Agreement between the measured and calculated results is satisfactory. It follows from the analysis that the de-

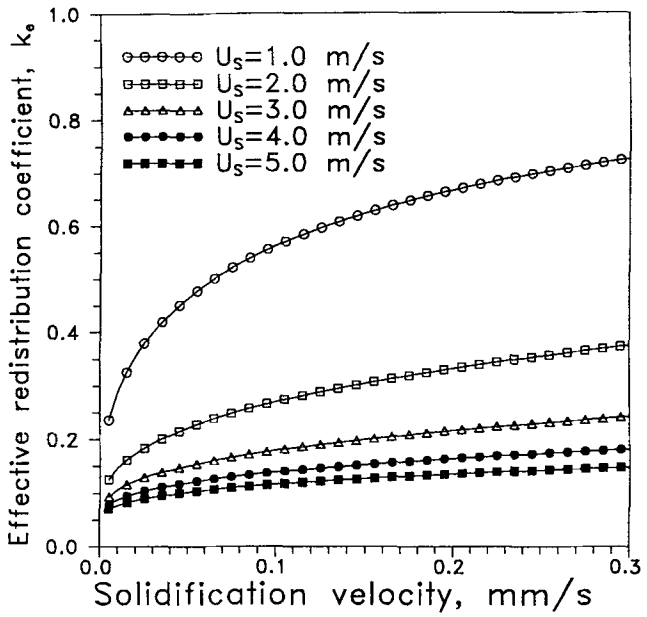

Fig. 11 Effect of solidification velocity on effective redistribution coefficient for various tangential velocities

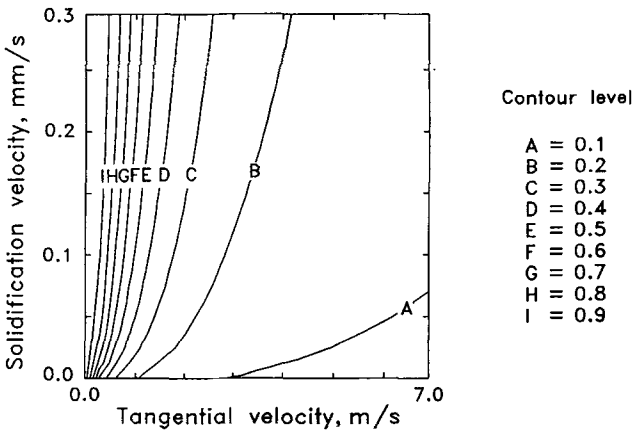

Fig. 12 Contours of effective redistribution coefficient at various solidification and tangential velocities

crease in the refining ratio of iron with increasing distance from the graphite pipe can be attributed to the increase in the tangential velocity, which in turn gives rise to the decrease in the effective redistribution coefficient. As solidification proceeds, however, the solute concentration in the liquid increases, and in turn the refining ratio increases. This effect is negligible in the earlier stage, but becomes important in the later stage.

5. Conclusions

- The effective redistribution coefficient decreases with decreasing solidification velocity and increasing tangential velocity.
- The diffusion boundary thickness is inversely proportional to the square root of the tangential velocity at a given solidification velocity.
- The calculated refining curves using the proposed effective redistribution coefficient are in good agreement with measured values.

Acknowledgments

This study has been supported by ChangSung and Korea Science Engineering Foundation through the Research Center for Thin Film Fabrication and Crystal Growing of Advanced Materials.

References

1. M. Kondo, H. Maeda, and M. Mizuguchi, *J. Met.*, Vol 11, 1990, p 36
2. Production of Extreme Purity Aluminum, U.S. Patent 4,222,830, 1980
3. Process of Purification of Metals, U.S. Patent 3,671,229, 1972
4. Purification Method of Aluminum, Japanese Patent Sho 59-50738, 1984
5. Purification Method of Aluminum, Japanese Patent Sho 59-41499, 1984
6. Process for Producing High-Purity Aluminum, U.S. Patent 4,469,512, 1984
7. J.A. Burton, R.C. Prim, and W.P. Slichter, *J. Chem. Phys.*, Vol 21, 1953, p 1987
8. L.O. Wilson, *J. Cryst. Growth*, Vol 44, 1987, p 247
9. V.G. Levich, *Physicochemical Hydrodynamics*, Prentice-Hall, 1962, p 90
10. V.J. Lunardini, *Heat Transfer in Cold Climates*, Van Nostrand Reinhold, 1981, p 611
11. E.A. Brandes, *Smithells Metal Reference Handbook*, Butterworths, London, 1983
12. E. Scheil, *Z. Metallkd.*, Vol 34, 1942, p 70